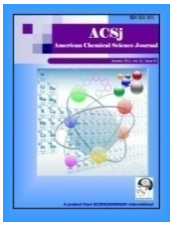

American Chemical Science Journal
5(2): 105-121, 2015, Article no.ACSj.2015.011
ISSN: 2249-0205

SCIENCEDOMAIN *international*
www.sciencedomain.org

Study of the Adsorption of Nitrogen Compounds for Diesel Fuel Production Using Three Commercial Materials

Pedro M. Vega-Merino[1,2*], Georgina C. Laredo[1], Fernando Trejo-Zárraga[2] and J. Jesús Castillo[1]

[1]Research Program of Transformation Processes, Mexican Petroleum Institute, 152 Lazaro Cardenas, Mexico D.F. 07730, Mexico.
[2]National Polytechnic Institute, CICATA-Legaria, 694 Legaria, Mexico D.F. 11500, Mexico.

Authors' contributions

This work was carried out in collaboration between all authors. Author PMVM carried out the experiments, performed the statistical analysis, wrote the protocol, and wrote the first draft of the manuscript. Author GCL designed the study and collaborated in the writing of the first draft of the manuscript. Author FTZ managed the literature searches and revised the manuscript. Author JJC collaborated in the experiments and managed the analyses of the study. All authors read and approved the final manuscript.

Article Information

DOI: 10.9734/ACSj/2015/13830
Editor(s):
(1) Nagatoshi Nishiwaki, Kochi University of Technology, Japan.
Reviewers:
(1) Anonymous, Jamia Millai Islamia Central University, India.
(2) Jerekias Gandure, Mechanical Engineering department, University of Botswana, Botswana.
(3) Mohammed Awwalu Usman, Department of Chemical Engineering, University of Lagos, Akoka, Yaba, Lagos, Nigeria.
Complete Peer review History: http://www.sciencedomain.org/review-history.php?iid=698&id=16&aid=6545

Original Research Article

Received 5th September 2014
Accepted 30th September 2014
Published 18th October 2014

ABSTRACT

The aim of this work was to study the removal of nitrogen (N-) compounds for ultra-low sulfur diesel (ULSD) production purposes by using three commercial materials: selexsorb® CDX (CDX), silica gel (SG), and activated carbon VG-077 (VG-077). The experiments were conducted in three steps: (1) Adsorption of quinoline, indole, or carbazole from model fuels (300wppm in a 1:1g/g n-hexadecane:toluene mixture) in a batch setup; adsorption of N- compounds from straight run gas oil (SRGO): (2) in a batch setup, and (3) in a fixed-bed column (FBC). Langmuir and Freundlich models were considered for modeling the adsorption isotherms of quinoline, indole, carbazole from model fuels and N-compounds from SRGO. Clark and Thomas models were employed for fitting the FBC

**Corresponding author: E-mail: pvega@imp.mx;*

experimental data. In the batch experiments, the adsorption capacities (q_m) for neutral N-compounds were 0.795mmol/g (VG-077), 0.287mmol/g (CDX), and for basic N-compounds were 0.708mmol/g (SG), 0.385mmol/g (CDX), and 0.242mmol/g (VG-077). The goodness of the fit for the Langmuir and Freundlich models strongly depended on the N-compound and the adsorbent when treating model fuels. Treating SRGO, VG-077 presented a higher q_m (0.855mmol/g) than the other two materials (0.687mmol/g (SG) and 0.372mmol/g (CDX)), which is understandable because neutral N-compounds represent 75% of nitrogen in this fuel. The Langmuir model was better than the Freundlich model to reproduce the adsorption isotherms properly with SRGO (R^2>0.9966). Besides, the pseudo second-order model performed better than the pseudo first-order model to simulate the adsorption rates in almost all cases, although the comparison was not straightforward, because the values depended highly on the N-compound and the material studied. In the FBC experiments, the Clark model agreed better with the experimental data than the Thomas model did. VG-077 achieved the highest N-adsorption (0.38mmol/g vs. 0.18mmol/g (SG) and 0.15mmol/g (CDX)). However, according to the preliminary estimation carried out, a higher adsorption capacity is still required for commercial application of this process.

Keywords: Adsorption; nitrogen; SRGO; batch; fixed-bed; activated-carbon; ULSD; modeling.

1. INTRODUCTION

The production of ultra-low sulfur diesel (ULSD) is very important for the environment protection. Therefore, many stringent environmental regulations for this nonrenewable fuel have been established worldwide in spite of the sustained decrement in the crude oil quality [1-3]. Moreover, when middle distillates are refined to produce ULSD, some fuel lubricity is lost. Minimum lubricity is required by the ASTM-D975 standard, which means oil companies must use either biodiesel or a synthetic additive to return fuel to its pre-ULSD lubricity level [4]. Several options have been developed for producing ULSD, for example: adsorption of nitrogen (N-) compounds from feedstocks used for diesel fuel production [5].

The N-compounds are classified into two groups: basic (e.g. pyridines, quinolines), and neutral (e.g. indoles, carbazoles) [6]. While the basic N-compounds have an inhibiting effect on the hydrodesulfurization (HDS) catalyst by being adsorbed on the acidic sites, the neutral N-compounds tend to form gums by polymerization, leading to pore plugging of these catalysts [7-10]. In a straight run gas oil (SRGO), indoles and carbazoles represent 75wt.% and quinolines 25wt.% of the N-concentration (300-400wppm) [11,12]. Thus, to elucidate the adsorption behavior on the adsorbents by N-compound type is very important.

The experiments of N-adsorption as a pretreatment step of the HDS process have been carried out in the liquid phase at ambient pressure and temperature [5]. Adsorption is an exothermic, spontaneous, reversible, and selective process that takes place without hydrogen consumption [13-15]. Some effective adsorbents have been used to denitrogenate diesel fuels: activated carbon, activated alumina, aluminosilicates, silica gel, mesoporous silica, metal-organic frameworks, ion exchange resins, and zeolites, among others [5]. The performance of these materials depended on the physical and chemical properties of the adsorbent, fuel being treated, and experimental conditions. Nevertheless, there is still a lack of studies dealing with real feedstocks in refinery settings.

In this work, three commercial adsorbents were chosen considering their reported adsorption characteristics. Silica gel (SG) and activated carbon (VG-077) have been widely used for N-adsorption towards ULSD production [5]. Selexsorb® CDX (CDX) is a promoted alumina-based adsorbent for refinery production processes [16]. The main objective of this work was to determine preliminary the practical feasibility of the N-removal for ULSD production using these commercial adsorbents by:

a) Carrying out experiments in batch and fixed-bed setups using model fuels and SRGO. The tests were conducted at given experimental conditions, which were established considering commercial HDS units as a reference.
b) Mathematically modeling the adsorption behavior observed with the model fuels and SRGO. That is, fitting the equilibrium data to the Langmuir and Freundlich models; estimating the kinetic data by the

pseudo first- and second- order rate equations; and using the Clark and Thomas models to predict the breakthrough curves [13,17-22].

c) Performing preliminary calculations to extrapolate the observed adsorption capacity towards a likely commercial application of this process.

The results of this work permitted the appropriate use of the proposed models to reproduce the experimental data in batch and fixed-bed setups. Many articles describe adsorption applications for the removal of N-compounds in batch mode but only few studies report fixed-bed experiments [15]. This approach allows to estimate a sustainable adsorption capacity of N-compounds for a commercial HDS unit producing ULSD.

2. MATERIALS AND METHODS

2.1 Materials

Quinoline, indole, and n-hexadecane were purchased from Sigma-Aldrich Co., and carbazole and toluene from Merck-Schuchardt Co. The reactants were utilized as such without further purification process. The adsorbent CDX was purchased from Almatis AC, Inc., SG from Merck-Schuchardt Co., and VG-077 from Clarimex. Three model fuels were obtained by dissolving: 277mg (2.14mmol) of quinoline, or 251mg (2.14mmol) of indole, or 358mg (2.14mmol) of carbazole in 100g of a toluene:n-hexadecane mixture (1:1g/g) for 300wppm of N-concentration. Henceforth, N-compound content will be considered as N-concentration. A sample of SRGO was kindly provided by PEMEX-Refining, México.

2.2 Characterization and Testing Methods

2.2.1 Surface properties

BET area and pore volume were determined by nitrogen adsorption with a Quantachrome Automated Gas Sorption System [23].

2.2.2 Measurement of the nitrogen concentration

Quinoline, indole and carbazole concentrations from model fuels were obtained through calibration curves prepared with each N-compound. The analysis was carried out in a Bruker 450-GC model gas chromatograph equipped with a pulsed photometric detector, using a BR-5 column (fs, 50m x 0.32mm, df=0.5μm). The carrier gas was helium (3mL/min). The following temperature program was applied: 50C (5min), then 5C/min to reach 150C (5min), and 25C/min to reach 280C (15min); Detector temperature=320C and Injector temperature=300C. On the other hand, the total N-concentration in SRGO was analyzed with an ANTEK equipment (ASTM D-4629). The coefficient of variation (*CV*) for both instruments was lower than 3 and established as:

$$CV = U = \frac{100\,s}{n\,M} \quad (1)$$

where: *U* is the uncertainty; *s* is the standard deviation; *n* is the number of samples (in this case, six); and *M* is the average value of the *n* samples.

2.2.3 Testing method for the batch setup

The three adsorbents were crushed, sieved through 200/400mesh and dried out in a conventional oven at 423K up to 24h before the tests. Those adsorbents were examined with the three model fuels and SRGO. The equilibrium and kinetic experiments were carried out in a flask with a water-bath jacket at the following conditions [24]: Temperature=303K, Pressure=0.078 MPa, and stirring rate=460rpm.

Equilibrium experiments were carried out by using 15mL of feed and equilibrium data were obtained by changing the adsorbent/feed ratio (*A/F*) from 0.02 to 0.12g/g and measuring the N-concentration after 60min had passed. Kinetic experiments were carried out by using 50mL of feed and kinetic data were supplied by experiments where an *A/F*=0.08g/g was used and the samples were taken after (1, 2, 3, 5, 10 and 15) min had passed.

2.2.4 Testing method for the fixed-bed setup

In each case, the adsorbent was crushed, sieved to 60/80mesh and loaded in a stainless steel column with an inside diameter=1.13cm, bed height=22 cm, and bed volume=22mL. Due to their different loading densities, the loaded amounts of adsorbents were: 13.9g (CDX), 11.5g (SG), and 7.0g (VG-077). Before feeding SRGO to the column, the solids were treated under a nitrogen flow of 50-100mL/min, heated up to 473K and kept at this temperature for 60min to remove the adsorbed moisture and other compounds which could influence the adsorptive performance. After this pretreatment step, the

temperature of the fixed-bed was reduced to 303K for the adsorption test. The fixed-bed adsorption tests were carried out as follows: SRGO was fed to the bottom of the column at a flow rate=1.84mL/min (Liquid hourly space velocity (*LHSV)=5h*$^{-1}$) regulated by a constant speed pump. The effluent samples from the top of the column were periodically collected for nitrogen analysis.

The adsorption loadings in the bed (q_{fb}, mmol/g) were obtained by multiplying the area *A* (ml/g) obtained by numerical integration of the fixed-bed column data (effluent volume versus *1 - C/C$_o$*) with the concentration of N-compounds in the feed (mmol/mL). A regression calculation from Polymath 6.1 professional–software was used for integration.

2.3 Mathematical Treatment of Data

2.3.1 Global mass balance

A global mass balance states the fact that the amount of nitrogen adsorbed on the solid must equal the amount of nitrogen removal from the model fuel or SRGO. In the equilibrium tests, the adsorption capacity was calculated from the existing difference between the initial and equilibrium concentrations of N-compounds. It is expressed mathematically as [18]:

$$q_e = \frac{C_o - C_e}{m} V \tag{2}$$

where: q_e is the equilibrium adsorption capacity given by the mass amount of adsorbed nitrogen per gram of adsorbent (mg/g); C_o and C_e are the initial and equilibrium N-concentrations in the liquid phase (mg/mL), respectively; *V* is the volume of fuel (mL); and *m* is the adsorbent mass (g).

In the kinetic tests, the adsorbed nitrogen at time *t* was calculated by Eq. (3) [18]:

$$q_t = \frac{C_o\ V_o - C_t\ V_t}{m} \tag{3}$$

where: q_t is the adsorption capacity at time *t* expressed in terms of the mass amount of adsorbed nitrogen per gram of adsorbent (mg/g); C_o and C_t are the nitrogen concentrations (mg/mL) and V_o and V_t are the volumes (mL) of the liquid phase at initial and *t* times, respectively; again, *m* is the adsorbent mass (g).

2.3.2 Equilibrium measurements

The adsorption isotherms of the N-compounds on the three materials were fitted to the Langmuir (Eq. 4) and Freundlich (Eq. 5) models in order to compare their results and establish the most appropriate option for a given case [13,17-19]:

$$q_e = \frac{q_m\ K_L\ C_e}{1 + K_L\ C_e} \tag{4}$$

$$q_e = K_F\ C_e^{\frac{1}{n}} \tag{5}$$

where for Eq. (4): q_e is the equilibrium adsorption capacity expressed by the molar amount of adsorbed nitrogen per gram of adsorbent (mmol/g); q_m is the adsorption capacity for a complete monolayer coverage, also defined by the molar amount of adsorbed nitrogen per gram of adsorbent (mmol/g); K_L is the Langmuir constant for the adsorption energy (the strength of the bond generated between the surface and the adsorbing species) (L/mmol); and C_e is the equilibrium N-concentration in the liquid phase (mmol/L). For Eq. (5): K_F (mmol$^{(1-1/n)}$L$^{(1/n)}$/g), and *n* (dimensionless) are the Freundlich parameters for the adsorptive capacity and intensity, respectively; likewise, q_e and C_e are those described in Eq. (4). A procedure of linear least-squares fitting was applied to estimate the adsorption parameters from the following plots: (*1/C$_e$* vs. *1/q$_e$*) for Eq. (4) and (*log(C$_e$)* vs. *log(q$_e$)*) for Eq. (5).

Considering the Langmuir model and in accordance with Almarri et al. [25] in their description of the activated carbon behavior on quinoline and indole adsorption, they defined the relative affinity (*RA, L/g*) of the adsorbents described by multiplying K_L, Q_m, and *S*:

$$RA = q_m\ K_L = K_L\ Q_m\ S \tag{6}$$

where: q_m *and* K_L are those cited in Eq. (4); Q_m is the maximum density of the adsorption sites per unit area (μmol/m^2), and *S* is the adsorbate-accessible surface (m^2/g, Table 1).

2.3.3 Kinetic measurements

The adsorption kinetics of the N-compounds was studied using pseudo first-order (Eq. 7) and pseudo second-order (Eq. 8) kinetic models as follows [19]:

$$\log (q_e - q_t) = \log q_e - \frac{k_{1ad}\ t}{2.303} \quad (7)$$

$$\frac{t}{q_t} = \frac{1}{k_{2ad}\ q_e^{\,2}} + \frac{t}{q_e} \quad (8)$$

where for Eq. (7): q_e is the final adsorption capacity expressed by the molar amount of the adsorbed nitrogen per gram of adsorbent (mmol/g); q_t is the adsorption capacity at contact time t and given by the molar amount of the adsorbed nitrogen per gram of adsorbent (mmol/g); k_{1ad} is the rate constant of pseudo first-order adsorption (1/min); and t is the contact time (min). For Eq. (8): k_{2ad} is the rate constant of pseudo second-order adsorption (g/(mmol min)). Again, t, q_t, and q_e are the variables described in Eq. (7). The experimental data were fitted to Eq. (7) and Eq. (8) to calculate the rate constants as follows: k_{1ad} from the slope of the ($log(q_e-q_t)$ vs. t) plot, and k_{2ad} from the intercept of the (t/q vs. t) plot.

2.4 Fixed-bed Measurements

2.4.1 Clark model

This mathematical model was initially developed by Clark [20] to predict the performance of a granular activated carbon-organic compound system. The Clark model was deduced based on the following assumptions: there are expressions for the liquid phase continuity and adsorption rate; the shape of the mass-transfer zone is constant and all the adsorbates are removed at the end of the column; and the isotherm fits the Freundlich type. The final expression of Clark model is:

$$\left(\frac{C_i^{n-1}}{1+Ae^{-rt}}\right)^{\frac{1}{n-1}} = C \quad (9)$$

$$A = \left(\frac{C_i^{n-1}}{C_b^{n-1}} - 1\right) e^{rt_b} \quad (10)$$

where for Eq. (9): C_i is the constant N-concentration in the feed (mg/L); n is the Freundlich constant for the intensity (dimensionless); A is a Clark parameter depending on N-concentrations, t and r (dimensionless); r is a Clark parameter which depends on n, the mass-transfer coefficient, flow rate of feed per unit of cross-sectional area, and the differential change of column height related to the differential change of service time (1/min); t is the service time (min); C is the effluent N-concentration at time t (mg/L). For Eq. (10): C_b is the breakthrough N-concentration (mg/L); and t_b is the breakthrough time (min). A, C_i, and r are those cited for Eq. (9).

Prior to using the Clark model, it is necessary to determine n by a batch test and to rearrange Eq. (9) into a linear form (the slope and intercept of the plot: ($ln[(C_i/C)^{n-1}-1]$ vs. t) allow one to solve r and A, respectively), and generate the whole breakthrough curve.

2.4.2 Thomas model

The Thomas model estimates the absorptive capacity of adsorbent and predicts the breakthrough curve, assuming the second-order reversible reaction kinetics and Langmuir isotherm. This model also predicts the adsorption process where external and internal diffusion resistances are extremely small [17-18,21-22]. The Thomas model is given by:

$$\ln\left(\frac{C_F}{C} - 1\right) = \frac{k_{Th}\ q_F\ m}{Q} - k_{Th}\ C_F\ t \quad (11)$$

where: C_F and C are the N-concentrations at equilibrium and effluent at time t, respectively (mg/L); k_{Th} is the Thomas rate constant (L/(min g)); q_F is the value of q in equilibrium with C_F (mg/g); m is the adsorbent mass loaded in the column (g); Q is the flow rate (L/min); and t is the service time (min). Having several pairs of m and Q, the values of k_{Th} and q_F can be derived through a plot of ($ln[(C_F/C)-1]$ vs. t).

3. RESULTS AND DISCUSSION

3.1 Characterization of the Adsorbents

3.1.1 BET area and pore volume

BET area decreased in the order of VG-077>SG>CDX (Table 1). Considering that the

Table 1. Textural properties of selexsorb® CDX (CDX), silica gel (SG), and activated carbon (VG-077)

Properties	CDX	SG	VG-077
BET area (m^2/g)	520	645	1270
Pore Volume (cm^3/g)	0.48	0.82	0.81

amount of nitrogen that a material can adsorb is proportional to the surface area, VG-077 would present the best performance in the adsorption tests.

Pore volume represents the total volume of the pores in a solid particle per unit weight of the solid. Some materials, like VG-077, contain a complex network of pores of various shapes and sizes. Those pores have an irregular geometry, are branched and interconnected by passages which may or may not be constricting [18]. According to the results, the pore volume decreased in the order of SG≈VG-077>CDX (Table 1).

3.2 Batch Experiments Treating Model Fuels

3.2.1 Adsorption isotherms

According to (Fig. 1), the adsorption of quinoline decreased in this order: SG>CDX>VG-077 (0.23-0.40mmol/g at N-concentrations at equilibrium of 6-9mmol/L). The adsorption of indole and carbazole diminished in the order of VG-077>CDX>SG (Figs. 2 and 3). The maximum adsorption of indole observed in these tests was about 0.80 to 0.20mmol/g at N- concentrations at equilibrium of 12-16mmol/L. The maximum adsorption of carbazole was of 0.02-0.12mmol/g at N-concentrations at equilibrium of 4-8mmol/L. The order of adsorption by N-compound type went for CDX and SG: quinoline>indole>carbazole and for VG-077 quinoline=indole>carbazole. As can be seen from (Fig. 1 to Fig. 3), VG-077 achieved the highest (indole+carbazole) adsorption (q_m=0.795mmol/g) and SG reached the highest quinoline adsorption (q_m=0.708mmol/g). CDX performed better than VG-077 adsorbing quinoline (0.312 vs. 0.228mmol/g, at C_e=7.65mmol/L), and better than SG adsorbing neutral N-compounds (0.153 vs. 0.051mmol/g at C_e=12.63mmol/L for indole, and 0.071 vs. 0.012mmol/g at C_e=5.822mmol/L for carbazole). That is, the N-adsorption depends on the material and N-compound being adsorbed.

In previous works, Kubelková and Jíru [26] reported that pyridine (a basic N-compound) was adsorbed on the "free" OH groups of the adsorbent by hydrogen bond interactions.

Kim et al. [27] studied the mechanism of the N-adsorption on Ni/SiO_2-Al_2O_3, activated alumina and activated carbon, using model fuels, and found that: the adsorptive selectivity of the activated alumina for quinoline was higher than that for indole due to an acid–base interaction; and there were many oxygen functional groups on the activated carbon surface, which could be separated into acidic groups (e.g. carboxyl and phenol groups), and basic groups (e.g. ketone and chromene groups). Quinoline may have a strong interaction with the acidic groups, while indole might interact with both the acidic and basic groups due to the weak acidity of the H bonded to the N atom and the weak basicity of the N atom in indole. Therefore, the activated carbon may show a higher adsorptive selectivity for indole than for quinoline [27].

According to Almarri et al. [25], oxygen functionalities over the activated carbon surface were important when adsorbing N-compounds; thus, the total concentration of the acidic functional groups, including carboxylic, anhydride, lactone and phenol groups have a direct effect on the increasing absorption of N-compounds. Almarri et al. [25] affirmed that indole was more adsorbed than quinoline on activated carbons: 0.40-1.26mmol/g of quinoline and 0.67-1.66mmol/L of indole both as nitrogen, depending on the type of activated carbon, when studying model fuels conformed by quinoline or indole in decane (16.4mmol/L as nitrogen).

The preferred adsorption of basic N-compounds over neutral N-compounds on alumino-silicate materials, was also observed by Liu et al. [28] after performing density functional theory studies. Additional studies regarding the material structure and adsorption behavior of these materials are in progress.

The values for the parameters of Langmuir and Freundlich models: K_L, q_m, K_F, and n are included in (Tables 2, 3 and 4). The excellent linear

correlation indicates that the adsorption of quinoline, indole, and carbazole on CDX follows the Langmuir adsorption isotherm, with correlation factors (R^2) higher than 0.985. In the case of SG, the Langmuir model only could describe the behavior of the quinoline adsorption, although the Freundlich model presented a better fit. Carbazole and indole adsorption were not fitted well by neither of the models in SG. In the case of VG-077, quinoline adsorption was better described by the Langmuir model. The indole adsorption was fitted almost equally well by both models and carbazole adsorption preferred the Freundlich model, with R^2>0.995. In the case of the Freundlich isotherms, a value of $(1/n)<1$ generally indicates that adsorption capacity is slightly suppressed at lower equilibrium concentrations.

According to the assumptions of the models [13,17-19], in the case of Langmuir behavior, the adsorption occurs at definite localized sites, each site binds only one molecule, there are no forces of interaction among adjacent adsorbed molecules, there is only one adsorption energy (one-type site), and just monolayer adsorption occurs. Therefore, this behavior applies mostly for the quinoline, indole and carbazole adsorption on CDX, and quinoline on VG-077. The Freundlich isotherm indicates that SG presents a highly heterogeneous surface in the adsorption of quinoline. The same could be said for indole and carbazole on VG-077. Furthermore, the Freundlich model does not predict saturation adsorption; infinite surface coverage is expected to occur, which may lead to a multilayer adsorption of these compounds on the surface of both materials. Similar result was found by Wen et al. [19].

Values of RA and Q_m are shown in (Tables 2, 3, and 4). SG presented the highest q_m value for quinoline, followed by CDX and VG-077. VG-077 presented the highest q_m value for indole followed by CDX. The highest q_m value for carbazole was presented by VG-077. Almarri et al. [25] described a carbon (*AC4*) capable of adsorbing 1.23mmol/g of nitrogen from quinoline and 1.38mmol/g of nitrogen from indole. The highest Q_m for quinoline was presented by SG, whereas VG-077 presented the highest Q_m for indole. CDX and VG-077 presented similar values of Q_m for carbazole. Thus, VG-077 showed the highest density for the adsorption of neutral N-compounds, and SG for basic N-compounds.

3.2.2 Adsorption kinetics

The adsorption rates of the N-compounds from the model fuels with the different materials are shown from (Figs. 4 to 6). By inspection, the major changes in the curves occurred in the first

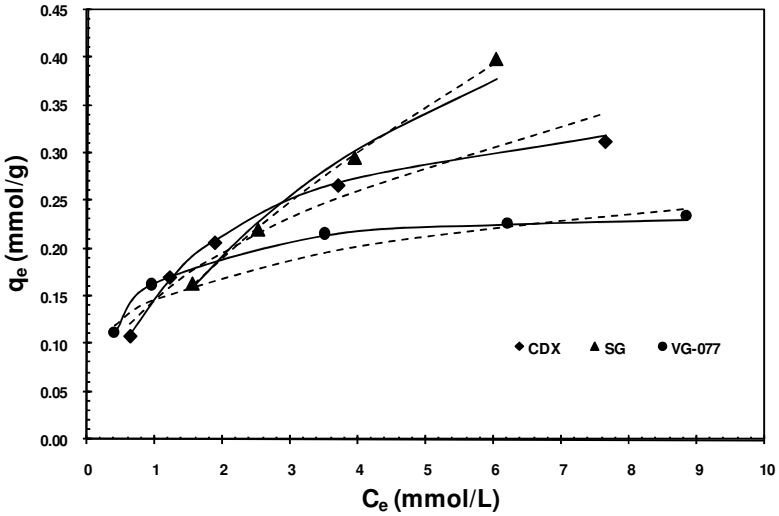

Fig. 1. Adsorption isotherms of quinoline on selexsorb® CDX (CDX), silica gel (SG), and activated carbon (VG-077). at 303K

(Langmuir (continuous lines) and Freundlich (discontinuous lines))

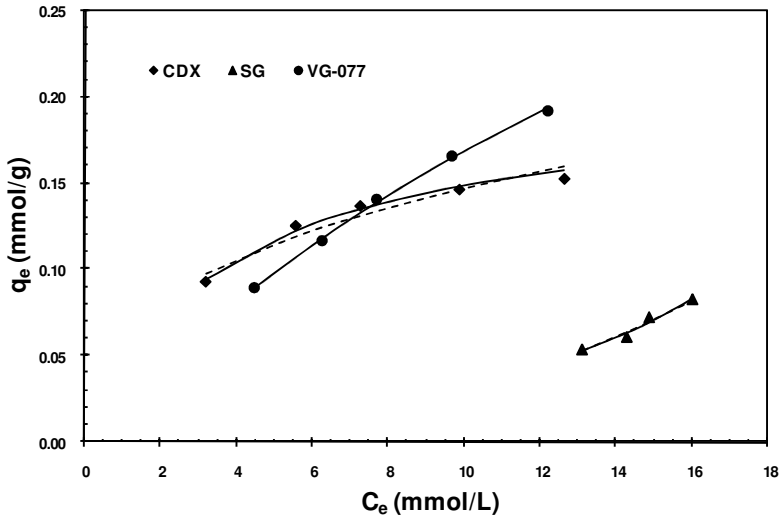

Fig. 2. Adsorption isotherms of indole on selexsorb® CDX (CDX), silica gel (SG), and activated carbon (VG-077) at 303K

(Langmuir (continuous lines) and Freundlich (discontinuous lines))

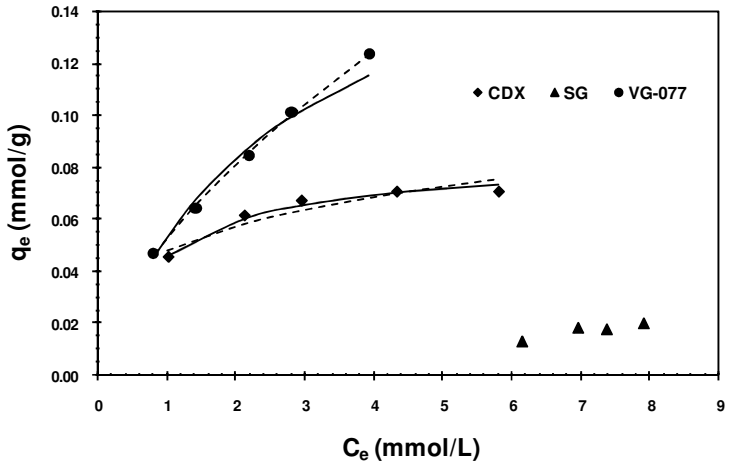

Fig. 3. Adsorption isotherms of carbazole on selexsorb® CDX (CDX), silica gel (SG), and activated carbon (VG-077) at 303K

(Langmuir (continuous lines) and Freundlich (discontinuous lines))

5min and it seems that only 10min were necessary to approach a steady-state condition for the adsorption of quinoline and indole on the three materials. However, it seems that more than 15min would be needed in the case of carbazole to reach the same condition. This performance agrees with the fact that larger molecules tend to diffuse more slowly from the liquid phase, needing longer times to achieve a steady-state condition [13].

The values of k_{1ad}, k_{2ad} and R^2 are included in (Tables 5, 6 and 7). These results show that the pseudo second-order model reproduces acceptably the adsorption rates of the N-compounds on the three adsorbents. Also, the goodness of the fit could be seen from (Figs. 4 to 6). A pseudo second-order kinetic behavior was also observed by Wen et al. [19] when adsorbing N-compounds from a model fuel on activated carbon, reporting a higher k_{2ad} for quinoline (0.417mmol/g/min) than for indole (0.267mmol/g/min), and carbazole

(0.264mmol/g/min. These results were associated to the fact that quinoline is a basic N-compound with a lone-pair of electrons, which introduces a significant dipole moment, enhances attractive forces and favors intraparticle diffusion [19].

According to (Tables 5, 6 and 7), the quinoline adsorption rates in terms of the k_{2ad} (all the diffusion parameters are lumped into a sole adsorption rate constant) decreased in the following order: SG>VG-077>CDX. The adsorption rates of indole decreased in the order: SG>CDX>VG-077 and of carbazole in the order: CDX≈VG-077>SG. That is, the adsorption rates of the N-compounds did not follow a tendency and depended strongly on the material. The adsorption rates of adsorbates are associated with internal structure of the materials, which may favor diffusion through channels and accessibility to the adsorption sites [17].

Table 2. Parameters of the Langmuir y Freundlich models in the adsorption of quinoline, indole, and carbazole on selexsorb® CDX (CDX)

Model	Quinoline	Indole	Carbazole
Langmuir			
q_m (mmol/g)	0.385	0.203	0.084
K_L (L/mmol)	0.626	0.272	1.186
R^2	0.9988	0.9893	0.9853
RA (L/g)	0.241	0.055	0.100
Q_m (µmol/m^2)	0.740	0.390	0.162
Freundlich			
1/n	0.416	0.359	0.256
K_F (mmol$^{(1-1/n)}$ L$^{(1/n)}$ /g)	0.147	0.065	0.048
R^2	0.9502	0.9415	0.8963

Table 3. Parameters of the Langmuir y Freundlich models in the adsorption of quinoline, indole, and carbazole on silica gel (SG)

Model	Quinoline	Indole	Carbazole
Langmuir			
q_m (mmol/g)	0.708	[a]	[a]
K_L (L/mmol)	0.189	[a]	[a]
R^2	0.9912	[a]	[a]
RA (L/g)	0.134	[a]	[a]
Q_m (µmol/m^2)	1.098	[a]	[a]
Freundlich			
1/n	0.659	2.254	[a]
K_F (mmol$^{(1-1/n)}$ L$^{(1/n)}$ /g)	0.121	0.0002	[a]
R^2	0.9990	0.9650	[a]

[a,] *Negative values*

Table 4. Parameters of the Langmuir y Freundlich models in the adsorption of quinoline, indole, and carbazole on activated carbon (VG-077)

Model	Quinoline	Indole	Carbazole
Langmuir			
q_m (mmol/g)	0.242	0.602	0.193
K_L (L/mmol)	2.194	0.039	0.378
R^2	0.9997	0.9991	0.988
RA (L/g)	0.531	0.023	0.073
Q_m (µmol/m^2)	0.191	0.474	0.152
Freundlich			
1/n	0.229	0.771	0.628
K_F (mmol$^{(1-1/n)}$ L$^{(1/n)}$ /g)	0.147	0.237	0.052
R^2	0.9406	0.9966	0.9988

Table 5. Rate constants of the pseudo first- and second- order models in the adsorption of quinoline, indole, and carbazole on selexsorb® CDX (CDX)

Model	Quinoline	Indole	Carbazole
Pseudo first-order			
k_{1ad} (1/min)	0.374	0.287	0.281
R^2	0.9661	0.7826	0.9127
Pseudo second-order			
k_{2ad} (g/(mmol min))	5.142	12.452	12.451
R^2	0.9999	0.9997	0.9995

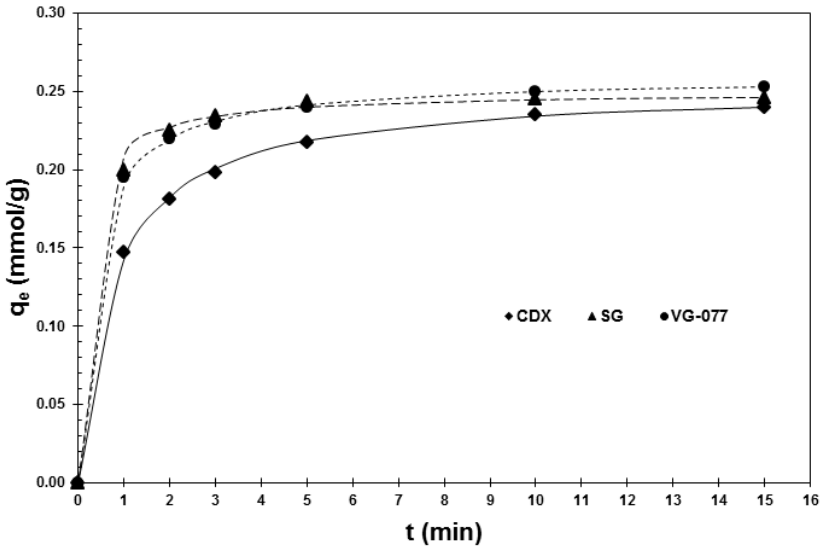

Fig. 4. Adsorption rates of quinoline on selexsorb® CDX (CDX), silica gel (SG), and activated carbon (VG-077) at 303K

(Pseudo second-order rate equation: different lines used for clarity purposes)

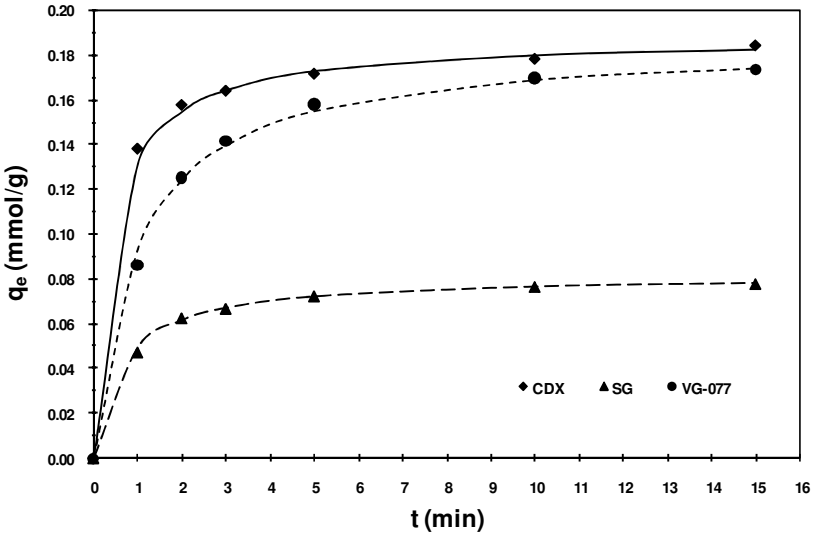

Fig. 5. Adsorption rates of indole on selexsorb® CDX (CDX), silica gel (SG), and activated carbon (VG-077) at 303K

(Pseudo second-order rate equation: different lines used for clarity purposes)

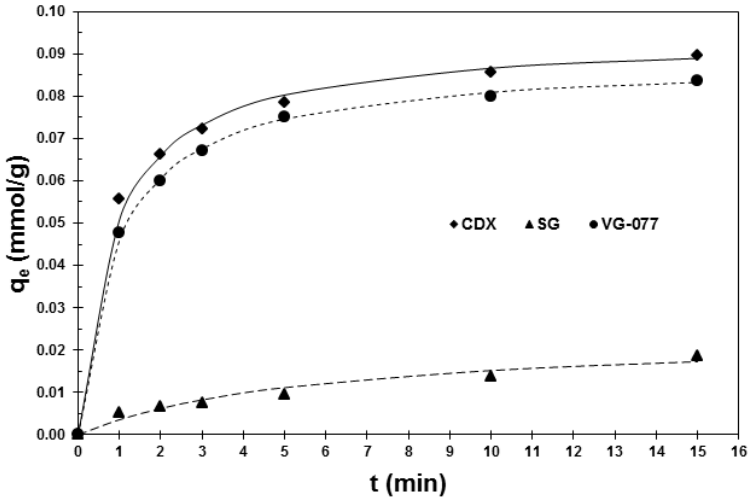

Fig. 6. Adsorption rates of carbazole on selexsorb® CDX (CDX), silica gel (SG), and activated carbon (VG-077) at 303K

(Pseudo second-order rate equation: different lines used for clarity purposes)

Table 6. Rate constants of the pseudo first- and second- order models in the adsorption of quinoline, indole, and carbazole on silica gel (SG)

Model	Quinoline	Indole	Carbazole
Pseudo first-order			
k_{1ad} (1/min)	0.511	0.379	0.125
R^2	0.8405	0.9422	0.9730
Pseudo second-order			
k_{2ad} (g/(mmol min))	20.086	18.881	7.361
R^2	0.9999	0.9999	0.9151

Table 7. Rate constants of the pseudo first- and second- order models in the adsorption of quinoline, indole, and carbazole on activated carbon (VG-077)

Model	Quinoline	Indole	Carbazole
Pseudo first-order			
k_{1ad} (1/min)	0.384	0.375	0.288
R^2	0.8907	0.9700	0.9122
Pseudo second-order			
k_{2ad} (g/(mmol min))	10.492	5.454	12.217
R^2	1.0000	0.9996	0.9998

3.3 Batch Experiments Treating SRGO

3.3.1 Adsorption isotherms

The adsorption of N-compounds from SRGO (380wppm; 0.851g/mL; 23.1mmol/L) on the adsorbents diminished in the order of VG-077>CDX=SG (Fig. 7). At approximately 14-15mmol/L of N-compound concentration at equilibrium, VG-077 adsorbed 0.45mmol/g, and CDX and SG: 0.20mmol/g. As it was seen in the model fuels, VG-077 was better for adsorbing neutral N-compounds; therefore, it is understandable that VG-077 presented a higher adsorption capacity than the other materials because 75% of the N-compounds from the SRGO are of this type [11,12]. Using activated carbons, Wen et al. [19] found an adsorption of 0.56-0.58mmol/g from a light cycle oil with 32mmol/L of N-compounds.

The adsorption isotherms of SRGO on the three adsorbents fitted the Langmuir and Freundlich models quite well. The R^2 values indicate that the Langmuir model behaved better than a Freundlich model with CDX and SG; but the

opposite situation was observed with VG-077 (Table 8). The adsorption capacity, according to the Langmuir equation decreased in the following order: VG-077>SG>CDX.

Values of *RA* and Q_m were also calculated (Table 8) [25]. The q_m according to the Langmuir equation decreased as follows: VG-077>SG>CDX. Besides, values of *RA* followed this order: VG-077>CDX>SG whereas the highest Q_m was presented by SG, followed by CDX and VG-077. These results imply that interactions are different in each adsorbent. More details regarding these interactions will be given in a future paper.

As can be seen in (Table 9), the R^2 values show that the N-adsorption of SRGO on the tested adsorbents followed a pseudo second-order model (Fig. 8). The results of fitting experimental data with the pseudo first-order model for the N-adsorption of SRGO on the solids are excluded in (Table 9) because of negative values for the constant k_{1ad} and R^2 lower than 0.95. This kinetic performance was also observed by Wen et al. [19], then, the pseudo second-order model may be used as a first approximation when describing the adsorption kinetics of N-compounds present in real fuels. The adsorption rates described by pseudo second-order model were: SG>CDX>VG-077.

3.3.2 Adsorption kinetics

Table 8. Parameters of the Langmuir and Freundlich models in the nitrogen adsorption on selexsorb® CDX (CDX), silica gel (SG), and activated carbon (VG-077) treating Straight Run Gas Oil (SRGO)

Model	CDX	SG	VG-077
Langmuir			
q_m (mmol/g)	0.372	0.687	0.855
K_L (L/mmol)	0.091	0.029	0.063
R^2	1.0000	1.0000	0.9966
RA (L/g)	0.034	0.020	0.054
Q_m (µmol/m^2)	0.715	1.065	0.673
Freundlich			
1/n	0.574	0.776	0.709
K_F (mmol$^{(1-1/n)}$ L$^{(1/n)}$ /g)	0.046	0.026	0.064
R^2	0.9920	0.9989	1.0000

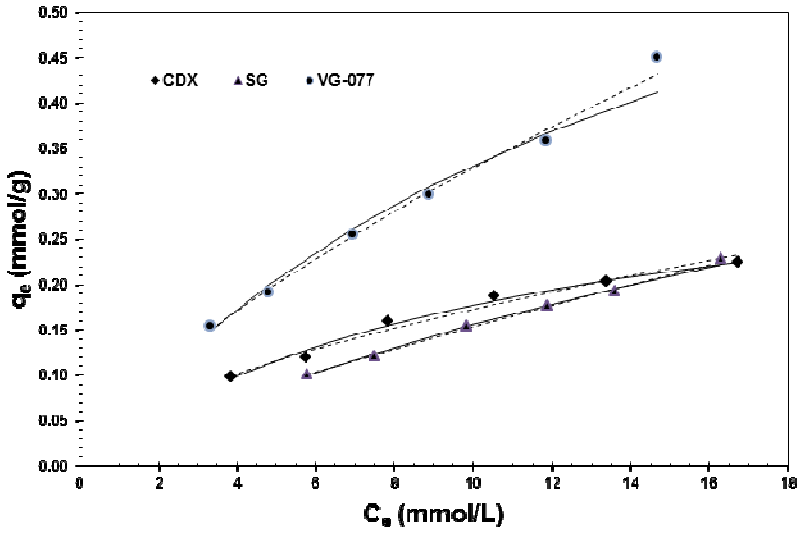

Fig. 7. Adsorption isotherms of SRGO on selexsorb® CDX (CDX), silica gel (SG), and activated carbon (VG-077) at 303K

(Langmuir (continuous lines) and Freundlich (discontinuous lines))

Table 9. Rate constant of the pseudo second-order model in the nitrogen adsorption on selexsorb® CDX (CDX), silica gel (SG), and activated carbon (VG-077) treating Straight Run Gas Oil (SRGO)

Model	CDX	SG	VG-077
k_{2ad} (g/(mmol min))	1.797	4.323	1.606
R^2	0.9992	0.9995	0.9995

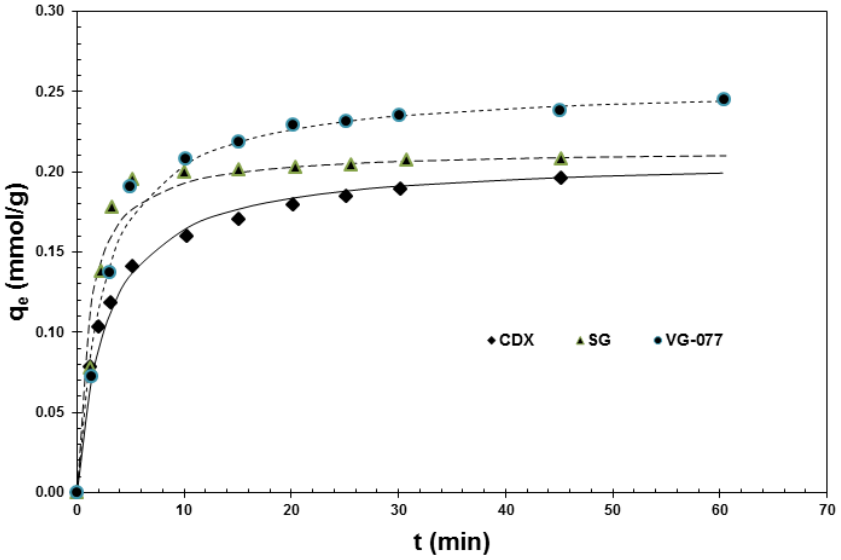

Fig. 8. Adsorption rates of SRGO on selexsorb® CDX (CDX), silica gel (SG), and activated carbon (VG-077) at 303K

(Pseudo second-order rate equation: different lines used for clarity purposes)

The rate constants (k_{2ad}) were smaller for the adsorption of N-compounds from SRGO than those for the model fuels (Tables 5-7, 9). These effects may be due to competitive adsorption among hydrocarbon families present in a real feed as SRGO.

3.4 Fixed-bed Experiments Processing SRGO

The experimental breakthrough curves of the evaluated adsorbents processing SRGO (380wppm, 23.1mmol/L) are shown in (Fig. 9). CDX was the first solid to show breakthrough at 0.72mL of treated SRGO per gram of adsorbent (mL/g). SG and VG-077 broke through at 0.87 and 2.90mL/g, respectively. After breakthrough, the C/C_o values (a ratio of the outlet N-concentration to the initial N-concentration in the SRGO) of CDX and SG increased sharply to 1.0 (saturation point) and more gradually for VG-077.

Taking VG-077 as a reference, the breakthrough amount of treated SRGO was about four and three times higher than those of CDX and SG, respectively. The amounts of treated SRGO corresponding to the saturation points by numerical integration of the experimental data were: 17.30mL/g (CDX), 23.90mL/g (SG), and 35.80mL/g (VG-077). Again, VG-077 presented the highest adsorption capacity (Table 10).

The breakthrough curves predicted by Clark and Thomas models are displayed in (Fig. 9). Results of fitting data with both models for the N-adsorption of SRGO on the solids are included in (Table 10). The R^2 indicates that the Clark model was the best option to simulate the performance of the evaluated adsorbents processing SRGO.

Several studies regarding the removal of N-compounds from SRGO using different materials by fixed-bed experiments have been described [29-32]. Sano et al., claimed an adsorption of 2.78mmol/g of N-compounds from a SRGO (N-concentration=15.9mmol/L) on activated carbon [29]; also, a N-compound adsorption between 0.71 and 2.14mmol/g from the same SRGO by

conventional activated carbons treated with HNO_3, H_2SO_4, and H_2O_2, followed by heat treatment [30]; and a removal of 0.43mmol/g from another SRGO (N-concentration=30.5mmol/L) on activated carbon fibers [31]. Besides, it was observed that clays removed organic nitrogen (0.08-0.14mmol/g) from a SRGO (N-concentration=151.3mmol/L), in tests conducted in a fixed-bed setup [32].

3.5 Estimation of the Commercial Application

Estimation of the feasibility of the SRGO pre-treatment in the ULSD production using the VG-077 tested in this work was carried out considering the following data: $LHSV$=1h^{-1}, Volume of adsorbent=165m^3; Liquid feed=SRGO, Density of SRGO=0.851ton/m^3, N-concentration of SRGO=380wppm; Adsorbent=VG-077, Loading density of VG-077=0.320ton/m^3, N-adsorption capacity of VG-077=0.38mmol/g.

At these conditions, preliminary calculations show that VG-077 would have a cycle length of 5.3h. It is further noticed that N-adsorption capacity of VG-077 appears to be low and is due primarily to the low breakthrough time. For practical cases, an adsorption system with multiple columns in series and countercurrent operation may warrant a consideration [33].

Table 10. Fitting parameters of Clark and Thomas models in the nitrogen adsorption on selexsorb® CDX (CDX), silica gel (SG), and activated carbon (VG-077) processing Straight Run Gas Oil (SRGO)

Model	CDX	SG	VG-077
Adsorption loading (mmol/g)	0.15	0.18	0.38
Clark model			
r (1/min)	-0.45	-0.31	-0.20
A	9.13	1.67	10.43
R^2	0.9972	0.9974	0.9986
Thomas model			
k_{Th} (L/(min g))	-1.48	-1.07	-0.72
q_E	-0.27	-0.41	-1.43
R^2	0.9933	0.9795	0.9885

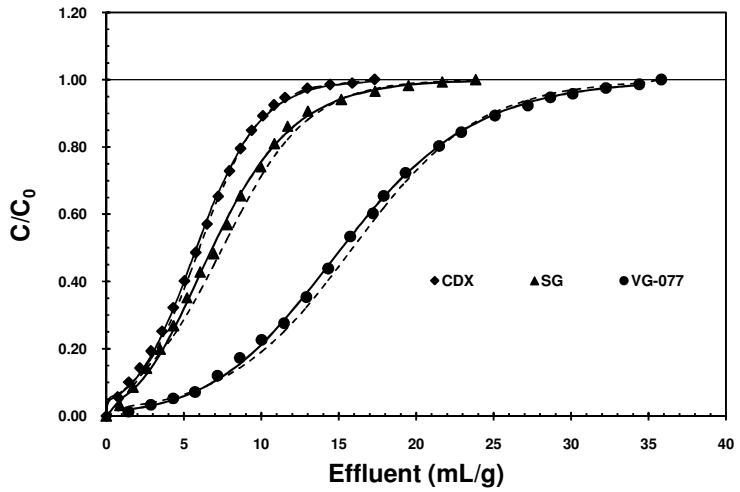

Fig. 9. Breakthrough curves of SRGO on selexsorb® CDX (CDX), silica gel (SG), and activated carbon (VG-077) at 303K

(Clark (continuous lines) and Thomas (discontinuous lines))

This could be a feasible option because an N-adsorption capacity of 1.73mmol/g is required to extend the cycle length from 5 to 24h without changing the adsorbent, increasing the adsorbent usage, decreasing the N-content of SRGO, and/or decreasing the feed rate. That is, an adsorbent must have an N-adsorption capacity five times greater than that achieved by VG-077 for a commercial application of this process. Increasing the cycle length to 24h or more, is also required to make the breakthrough time longer than the regeneration time.

Clearly, the required N-adsorption capacity enhances if *LHSV* changes from 1 to $2.5h^{-1}$, the volume of adsorbent decreases from 165 to $65m^3$, and/or the N-concentration of SRGO increases from 380 to >400wppm. This last case applies for several HDS units still producing low sulfur diesel (total S-concentration around 300wppm).

4. CONCLUSION

The results of this study show that the adsorption of N-compounds depends dominantly on the physical and chemical properties of the material and fuel being treated. VG-077 achieved the highest adsorption of neutral N-compounds (indole and carbazole) and SG reached the highest adsorption of basic N-compounds (quinoline). CDX performed better than VG-077 adsorbing quinoline and better than SG adsorbing neutral N-compounds.

The equilibrium experiments carried out in a batch setup with model fuels showed that the best fit for the experimental data either with Langmuir and Freundlich models varied with the N-compound being adsorbed and the material. Pseudo second-order rate equations fitted better the experimental data when using model fuels, but the absorption rate also depended strongly on the N-compound and material involved.

Equilibrium experiments performed with SRGO showed that the Langmuir model agreed better with the CDX and SG experimental data, while the Freundlich model was suitable for the VG-077, which presented the highest adsorption capacity. A pseudo second-order rate equation was a good fit for the N-compound adsorption data for all the materials.

Related to the experiments carried out in the fixed-bed column, it was evident that the Clark model exhibited a better performance than the Thomas model reproducing the breakthrough curves of the adsorbents processing SRGO. In this work, the activated carbon VG-077 achieved the highest total N-adsorption capacity at the established experimental conditions.

However, it is necessary to develop new adsorbents with a higher N-adsorption capacity in order to enhance adsorption of neutral N-compounds and make the breakthrough time longer if a commercial application of this adsorption process is being planned.

ACKNOWLEDGEMENTS

The authors express their sincere gratitude to the Instituto Mexicano del Petróleo (IMP) from México for the financial support of this study. Besides, Pedro M. Vega-Merino is gratefully indebted with IMP for his PhD scholarship.

COMPETING INTERESTS

Authors have declared that no competing interests exist.

REFERENCES

1. Stanislaus A, Marafi A, Rana MS. Recent advances in the science and technology of ultra low sulfur diesel (ULSD) production. Catal Today. 2010;153:1-68.
2. Topsøe H, Egeberg RG, Knudsen KG. Future challenges of hydrotreating catalyst technology. Prepr-Am Chem Soc Div Fuel Chem. 2004;49:568-9.
3. Song C. An overview of new approaches to deep desulfurization for ultra-clean gasoline, diesel fuel and jet fuel. Catal Today. 2003;86:211-63.
4. Anonymous. Ultra-low-sulfur diesel anything to worry about? Accessed 17 September 2014. Available: http://www.trawlerforum.com/forums/s6/ultra-low-sulfur-diesel-anything-worry-about-4473.html.
5. Laredo GC, Vega-Merino PM, Trejo-Zárraga F, Castillo J. Denitrogenation of middle distillates using adsorbent materials towards ULSD production: A review. Fuel Process Technol. 2013;106:21-32.
6. Girgis MJ, Gates BC. Reactivities, reaction networks, and kinetics in high-pressure catalytic hydroprocessing. Ind Eng Chem Res. 1991;30:2021-58.

7. Dong D, Jeong S, Massoth FE. Effect of nitrogen compounds on deactivation of hydrotreating catalysts by coke. Catal Today. 1997;37:267-75.
8. Ramachandran R, Massoth FE. The effects of pyridine and coke poisoning on benzothiophene HDS over cobalt-molybdenum/alumina catalyst. Chem Eng Commun. 1982;18:239-54.
9. Muegge B, Massoth FE. Catalyst Deactivation. Bartholomew CH, Butt JB, editors. Amsterdam: Elsevier. 1991;297-304.
10. Furimsky E, Massoth FE. Deactivation of hydroprocessing catalyst. Catal Today. 1999;52:381-495.
11. Laredo GC, Leyva S, Álvarez R, Mares MT, Castillo J, Cano JL. Nitrogen compounds characterization in atmospheric gas oil and light cycle oil from a blend of Mexican crudes. Fuel. 2002;81:1341-50.
12. Adam F, Bertoncini F, Dartiguelongue C, Marchand K, Thiebaut D, Hennion M. Comprehensive two-dimensional gas chromatography for basic and neutral nitrogen speciation in middle distillates. Fuel. 2009;88:938-46.
13. Ruthven DM. Principles of adsorption and adsorption processes. New York: Wiley Interscience; 1984.
14. Ali I. The quest for active carbon adsorbent substitutes: inexpensive adsorbents for toxic metal ions removal from wastewater. Separation & Purification Reviews. 2010;39,3-4:95-171.
15. Ali I. Water treatment by adsorption columns: evaluation at ground level. Separation & Purification Reviews 2014;43,3:175-205.
16. Anonymous. SELEXSORB CDX. Accessed 18 July 2014. Available: http://www.basf.com/group/corporate/en_GB/brand/SELEXSORB.
17. Noll KE, Gounaris V, Hou WS. Adsorption technology for air and water pollution control. USA: Lewis Publish; 1992.
18. Cooney DO. Adsorption design for wastewater treatment. USA: Lewis Publish; 1999.
19. Wen J, Han X, Lin H, Zheng Y, Chu W. A critical study on the adsorption of heterocyclic sulfur and nitrogen compounds by activated carbon: Equilibrium, kinetics and thermodynamics. Chem Eng J. 2010;164:29-36.
20. Clark RM. Evaluating the cost and performance of field-scale granular activated carbon systems. Environ Sci Tecnol. 1987;21:573-80.
21. Ghasemi M, Keshtkar AR, Dabbagh R, Safdari SJ. Biosorption of uranium (VI) from aqueous solutions by Ca-pretreated Cystoseira indica alga: Breakthrough curves studies and modeling. J Hazard Mater. 2011;189:141-9.
22. Xu Z, Cai JG, Pan BC. Mathematically modeling fixed-bed adsorption in aqueous systems. Appl Phys & Eng. 2013;14(3):155-76.
23. Barrett EP, Joyner LG, Halenda PP. Determination of pore volume and area distribution in porous substances. I Computations from Nitrogen Isotherms. J Am Chem Soc. 1951;73:373-80.
24. Vega Merino PM, Trejo Zárraga F, Laredo Sánchez GC. Estimación de parámetros de operación para la adsorción de compuestos orgánicos de nitrógeno de un gasóleo ligero primario utilizando un adsorbente comercial. México DF: CICATA-IPN; 2012. Español.
25. Almarri M, Ma X, Song C. Role of surface oxygen-containing functional groups in liquid-phase adsorption of nitrogen compounds on carbon-based adsorbents. Energy Fuels. 2009;23:3940–7.
26. Kubelková L, Jíru P. Study of the nature of silica gel active centers for water adsorption by infrared spectroscopy. Interaction with pyridine-water mixture. Collect Czech Chem Commum. 1972;37:2853-7.
27. Kim JH, Ma X, Zhou A, Song C. Ultra-deep desulfurization and denitrogenation of diesel fuel by selective adsorption over three different adsorbents: A study on adsorptive selectivity and mechanism. Catal Today. 2006;111:74-83.
28. Liu D, Gui J, Sun Z. Adsorption structures of heterocyclic nitrogen compounds over Cu(I)Y zeolite: a first principle study on mechanism of the denitrogenation and the effect of nitrogen compounds on adsorptive desulfurization. J Mol Cat A: Chem. 2008;291:17-21.
29. Sano Y, Choi K, Korai Y, Mochida I. Adsorptive removal of sulfur and nitrogen species from a straight run gas oil over activated carbons for its deep HDS, Appl. Catal., B 49. 2004;219–25.
30. Sano Y, Choi K, Korai Y, Mochida I. Selection and further activation of activated

carbons for removal of nitrogen species in gas oil as a pretreatment for its deep HDS, Energy Fuels 18. 2004;644-51.
31. Sano Y, Sugahara K, Choi K, Korai Y, Mochida I. Two-step adsorption process for deep desulfurization of diesel oil, Fuel 84. 2005;903–10.
32. de Figueiredo MAG, Zotin FZ, da Silva Júnior PF, Meirelles SL, Corrêa1 HL, Pinto BE, et al. Nitrogen compound removal for metropolitan diesel: Procedures for adsorbent regeneration, 2nd Mercosur Congress on Chemical Engineering. 4th Mercosur Congress on Process Systems Engineering; 2005.
33. Slejko FL. Adsorption technology: A step-by-step approach to process evaluation and application. New York and Basel: Marcel Dekker, Inc.; 1985.

Peer-review history:
The peer review history for this paper can be accessed here:
http://www.sciencedomain.org/review-history.php?iid=698&id=16&aid=6545